Evaluation of Luminescence Decay Measurements Probed on Pure and Doped Pt(IV) Hexahalogeno Complexes. II. Molecular Properties Obtained from Temperature Dependent Lifetime Curves

Ingo Biertümpel and Hans-Herbert Schmidtke

Institut für Theoretische Chemie, Heinrich-Heine-Universität Düsseldorf, Universitätsstr. 1, D-40225 Düsseldorf, Germany

Z. Naturforsch. **52a**, 447–456 (1997); received January 22, 1997

Lifetime measurements down to nearly liquid helium temperatures are used for determining energy levels and transition rates between excited levels and relaxations into the ground state. Energies are obtained from temperature dependent lifetimes by fitting experimental curves to model functions pertinent for thermally activated processes. Rates are calculated from solutions of rate equations. Similar parameters for pure and doped Pt(IV) hexahalogeno complexes indicate that excited levels largely belong to molecular units. Some of the rates between excited states are only somewhat larger than decay rates into the ground state, which is a consequence of the polyexponential decay measured also at low temperature (2 K). In the series of halogen complexes, the rates between spinorbit levels resulting from $^3T_{1g}$ increase from fluorine to bromine, although energy splittings become larger. Due to the decreasing population of higher excited states in this series, K_2PtF_6 shows a tri-exponential, K_2PtCl_6 a bi-exponential and K_2PtBr_6 a mono-exponential decay. In the latter case the population density of higher excited states relaxes so fast that emission occurs primarily from the lowest excited $\Gamma_3(^3T_{1g})$ level. Phase transitions and emission from chromophores on different sites can also be observed.

Key words: Pt(IV) complexes, luminescence decay, temperature dependence.

Introduction

A discussion of lifetime results obtained from emission spectra is based on reliable evaluations of measured decay curves. In the preceding article [1] (referred to as I in the following) the importance of statistical methods is outlined which allow a quality check of lifetime parameters obtained from luminescence decay measurements. Only if all statistical tests support non-rejection of model functions assumed in the starting hypothesis, the results can be used for physical interpretations. In case one of the various test statistics fails, the hypothesis is to be dismissed and another trial function must be chosen for fitting the measured lifetime curve which is expected to be more appropriate for simulating the radiative decay. Some procedures for obtaining suitable hypothesis functions have been demonstrated in I, using lifetime results on various Pt(IV) hexahalogeno complexes as appropriate examples.

The intensity of light emission, decaying with time, depends on several external parameters which ought to be specified for characterizing a lifetime curve: these are the length of the excitation pulse t_{exc}, the wavenumbers of excitation $\tilde{\nu}_{exc}$ and, for more detailed interpretation, of light detection $\tilde{\nu}_{det}$ where the emission is monitored. Most instructive is, in addition, the temperature dependence of lifetimes, which will be the main object in this part of the investigation.

Each of the exponentials in the time function simulating the decay experiments exhibits a different temperature dependence supplying informations on the emitting levels in the system. This is exemplified by temperature dependent lifetime measurements on some of the Pt(IV) systems as listed in Table 1 of I. Since the decay parameters of pure and doped complexes have been shown to be remarkably similar (see results on K_2PtCl_6 and Rb_2PtCl_6 compared to their

Reprint requests to Prof. Dr. H.-H. Schmidtke.

0932-0784 / 97 / 0500-0447 $ 06.00 © – Verlag der Zeitschrift für Naturforschung, D-72027 Tübingen

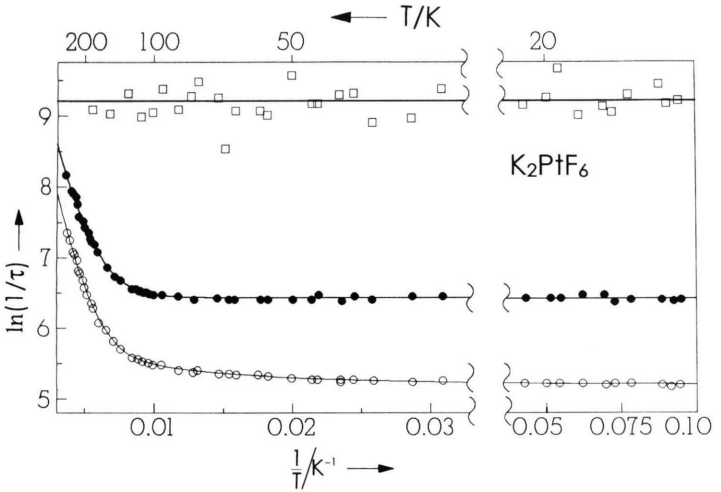

Fig. 1. Temperature dependence (Arrhenius plots) of decay constants τ_i for K_2PtF_6 ($\lambda_{exc} = 488$ nm, $\lambda_{det} = 675$ nm). Experimental data are o for the long time component τ_1, ● short time component τ_2, □ for the temperature independent component τ_3. The solid lines are the calculated curves from the fit.

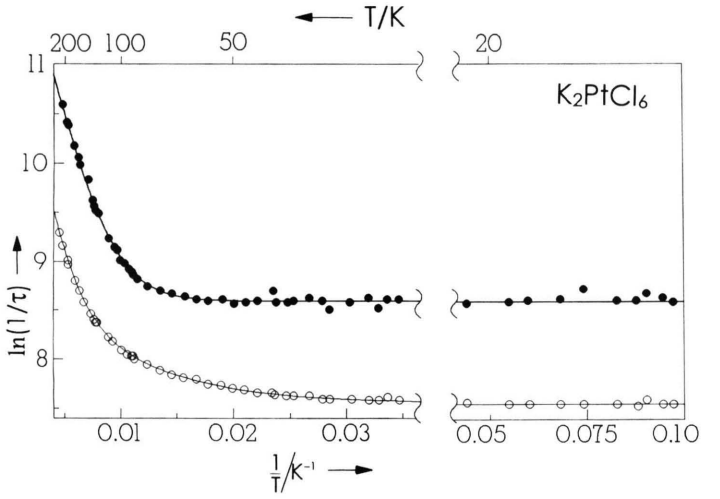

Fig. 2. Arrhenius plots for K_2PtCl_6 ($\lambda_{exc} = 514.5$ nm, $\lambda_{det} = 647$ nm). The symbols are explained in Figure 1.

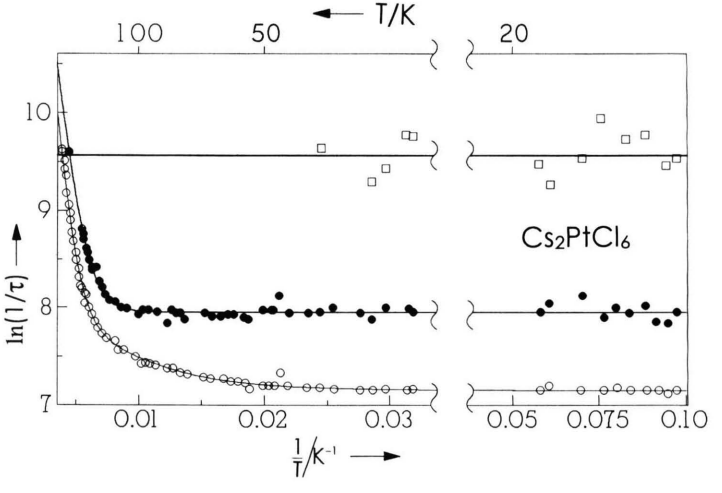

Fig. 3. Arrhenius plots for Cs_2PtCl_6 ($\lambda_{exc} = 514.5$ nm, $\lambda_{det} = 701$ nm). The symbols are explained in Figure 1.

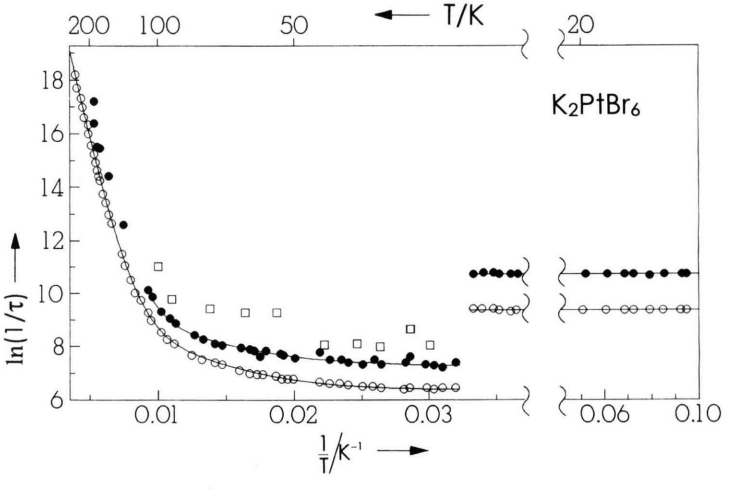

Fig. 4. Arrhenius plots for K_2PtBr_6 ($\lambda_{exc} = 514.5$ nm, $\lambda_{det} = 730$ nm). The symbols are explained in Figure 1.

respective doped systems in I), we safely can exclude levels to be involved which result from imperfections, traps or delocalization of electronic levels. We therefore can assume that photophysical rates of thermally activated processes, obtained from fitting temperature dependent lifetime curves, furnish at least preliminary data on seperated molecules in the crystals, i. e. on excited states, their degeneracies and relative transition rates belonging primarily to the complex molecules (see discussion in I). In general, these results are not easily available from other measurements, e. g. from absorption spectra, due to unadequate resolution. Energies and degeneracies could be compared with levels obtained from quantum chemical calculations. Assignments to different energy levels are confirmed by time resolved luminescence spectra exhibiting specific shifts of peak intensities. In one case, the results indicate the presence of different bromo complexes located on non-equivalent sites in the crystal, also a phase transition at low temperature becomes apparent from discontinuities in the temperature curves of lifetimes.

All experiments are carried out with the equipment already described in I.

Results

Radiative lifetimes were measured from microcrystalline Pt(IV) compounds reported in I at temperatures between 11 K and room temperature. The intensities (photon counts) were monitored at the respective maximum of emission. At each temperature the decay curve is fitted to linear combinations of exponentials using (12) and (13) of I. The fitting procedure supplies time constants τ_i and amplitudes A_i and B_i, valid for this temperature. The results were checked by test statistics; all prove values obtained are within the limits for non-rejection of the hypothesis function (see I). Separate evaluations of rise time and decay periods supplied identical sets of time constants within the time resolution available from the equipment.

The temperature dependence of each of the time constants τ_i is illustrated by $\ln(1/\tau_i) - 1/T$ plots, from which some of them are given in Figs. 1 to 4. Except for K_2PtBr_6, the temperature dependence of lifetimes supplies in all cases steadily varying functions with temperature differing for each τ_i. While the longer living components τ_1 and τ_2 show a strong temperature dependence at higher temperature, the

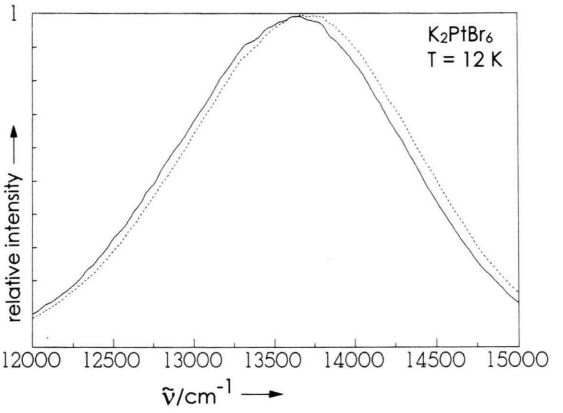

Fig. 5. Time resolved luminescence spectrum of K_2PtBr_6 (λ_{exc} = 454.5 nm). Short time spectrum (0 - 50μs): doted line, long time spectrum (200 - 300μs): solid line.

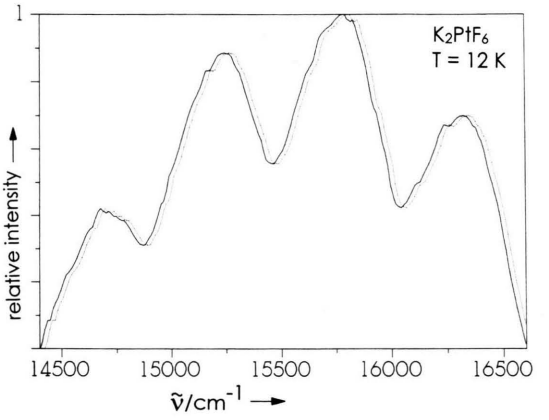

Fig. 6. Time resolved luminescence spectrum of K_2PtF_6 (λ_{exc} = 454.5 nm). Plots are as in Figure 5.

short living component τ_3, when observable, does not exhibit a temperature course in the entire region investigated. At lower temperatures (< 30 K), all lifetimes proved to be temperature independent within the accuracy of measurements. At temperatures > 90 K, all τ_1 and τ_2 plots exhibit a substantial increase of $1/\tau$.

In Fig. 5 and 6, time resolved luminescence spectra of two of the complexes are shown. The short time spectrum, recorded during the first 50 μs after turning off the excitation pulse, has its intensity maximum at higher energy compared to the long time spectrum, which is monitored within the time interval between 200 and 300 μs. This shift is not large but well defined in view of the fact that the bands are relatively broad showing no further resolution.

Table 1. Parameter fits to the Arrhenius plots. The rates $k_{i\,\mathrm{lim}}$ and coefficients s_l are given in s^{-1}, the activation energies ΔE_l in cm^{-1}, mean deviations in brackets.

Compound	i^a	$k_{i\,\mathrm{lim}} = \tau_{i\,\mathrm{lim}}^{-1}$	s_1	ΔE_1	s_2	ΔE_2	s_3	ΔE_3
K_2PtF_6	1:L	$1.8 \cdot 10^2$	$1.4 \cdot 10^2$	71(2)	$2.7 \cdot 10^4$	569(7)	—	—
	2:S	$6.3 \cdot 10^2$	$3.9 \cdot 10^4$	495(8)	—	—	—	—
K_2PtCl_6	1:L	$1.9 \cdot 10^3$	$4.9 \cdot 10^3$	97(3)	$1.3 \cdot 10^5$	425(9)	—	—
	2:S	$5.4 \cdot 10^3$	$3.0 \cdot 10^5$	320(9)	—	—	—	—
Rb_2PtCl_6	1:L	$1.6 \cdot 10^3$	$3.8 \cdot 10^3$	99(3)	$1.8 \cdot 10^6$	649(14)	—	—
	2:S	$4.0 \cdot 10^5$	$1.4 \cdot 10^5$	444(15)	—	—	—	—
Rb_2SnCl_6:Pt^{4+b}	1:L	$1.4 \cdot 10^3$	$2.1 \cdot 10^3$	102(4)	$2.1 \cdot 10^5$	624(14)	—	—
	2:S	$3.5 \cdot 10^5$	$3.4 \cdot 10^5$	338(15)	—	—	—	—
Rb_2SnCl_6:Pt^{4+c}	1:L	$1.3 \cdot 10^3$	$1.5 \cdot 10^3$	70(2)	$4.6 \cdot 10^4$	487(9)	—	—
Rb_2SnCl_6:Pt^{4+d}	1:L	$1.3 \cdot 10^3$	$1.5 \cdot 10^3$	82(5)	$4.2 \cdot 10^4$	~500	—	—
Cs_2PtCl_6	1:L	$1.3 \cdot 10^3$	$3.3 \cdot 10^3$	131(5)	$2.2 \cdot 10^6$	944(20)	—	—
	2:S	$2.9 \cdot 10^3$	$1.4 \cdot 10^6$	747(18)	—	—	—	—
K_2PtBr_6	1:A[e]	$5.8 \cdot 10^2$	$3.0 \cdot 10^4$	162(3)	$2.8 \cdot 10^8$	853(17)	$4.4 \cdot 10^{11}$	1535(10)
	2:B[e]	$1.4 \cdot 10^3$	$4.2 \cdot 10^4$	146(5)	$7.5 \cdot 10^8$	816(18)	$>10^{11}$	>1500
Rb_2PtBr_6	1:L	$8.5 \cdot 10^3$	$1.2 \cdot 10^4$	50(6)	$\sim 1.0 \cdot 10^8$	~ 800	—	—
Cs_2PtBr_6	1:L	$7.1 \cdot 10^3$	$\sim 1.0 \cdot 10^4$	~ 60	$\sim 1.0 \cdot 10^8$	>500	—	—

[a] L long, S short time decay components; concentrations of doped complexes are [b] 1.5 - 2.0%, [c] 0.5 - 0.7%, [d] 0.2-0.4%; [e] emission from non-equivalent sites in the lattice.

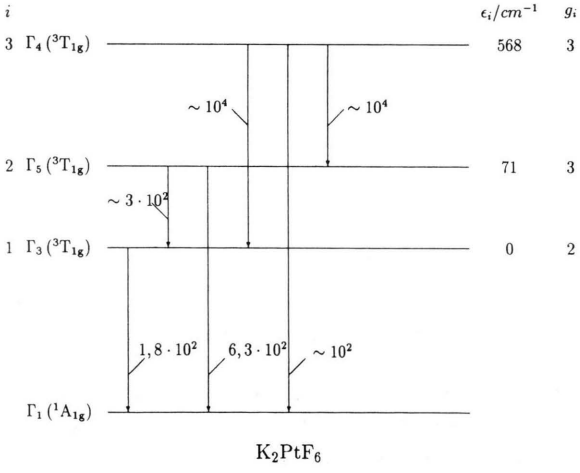

Fig. 7. Energy level scheme for K_2PtF_6 with energy differences $\varepsilon_i \equiv \Delta E_i$, degeneracy numbers g_i and transition rates k_{im} obtained from adaptation to the experimental data.

Discussion

1. Low Temperature Region

In the region where the lifetimes are in fact temperature independent, the discussion of the decay kinetics is straightforward. At low temperature, thermal population of higher electronic levels and therefore thermally activated decay is not possible. Emission only results from the lowest excited level with the lifetime constant $\tau_{1\,\mathrm{lim}}$ which is the long time component τ_1. The corresponding rate constant for this emission is $k_{1\,\mathrm{lim}} = 1/\tau_{1\,\mathrm{lim}}$, where $k_{1\,\mathrm{lim}}$ is identical with k_{10} in Figure 7. Assignment of the long time component to the lowest emitting state is supported by time-resolved spectra in which the long time spectral bands belong to lower energy than the short time spectra (cf. Fig. 5 and 6). The $k_{1\,\mathrm{lim}}$ values obtained for the compounds investigated are compiled in Table 1.

The measured lifetime τ close to zero temperature largely corresponds to the natural (intrinsic) lifetime τ_0 which represents the radiative part of decay with the rate k_{rad} in

$$\frac{1}{\tau} = k_{\mathrm{rad}} + k_{\mathrm{nrad}}. \tag{1}$$

The non-radiative part is further partitioned into intra- and intermolecular rates as

$$k_{\mathrm{nrad}} = k_{\mathrm{nrad}}(\mathrm{intra}) + k_{\mathrm{nrad}}(\mathrm{inter}). \tag{2}$$

In addition, other photophysical or photochemical processes may act as decay channels.

We therefore can assume that non-radiative contributions are relatively small at low temperature. The

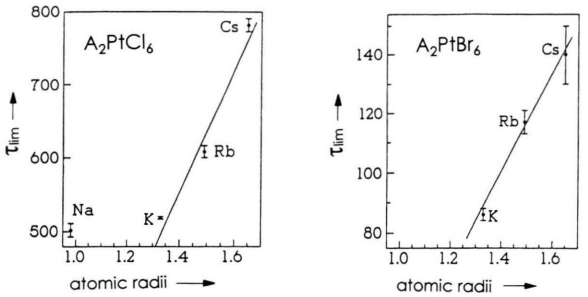

Fig. 8. Low temperature lifetimes (longtime component $\tau_{l\,lim}$) of hexahalogeno Pt(IV) complexes vs. ionic radii of counter ions (see text). The solid line is from the linear regression.

intramolecular parts are known to be negligible if the electronic energy gap between the emitting state and the ground level is large (in our case $> 15000\,cm^{-1}$) and is bridged by a large number (25 to 70) of vibrational quanta [2], which are $214\,cm^{-1}$ for K_2PtBr_6 and $600\,cm^{-1}$ for K_2PtF_6. For Cr(III) amine complexes, e. g., 5 to 6 N-H vibrational quanta bridging the electronic gap are sufficient to explain the k_{nrad} rate constants which amount almost entirely to the measured total rates (very small quantum yields [3, 4]), i. e. for larger gaps k_{rad} should become dominant. Intermolecular non-radiative transitions are, however, finite: in the series of hexachloro- and hexabromo-Pt(IV) complexes with different alkali ions a change of long living lifetime components $\tau_{l\,lim}$ is well observed (cf. Table 1 of I). A plot against atomic (Goldschmitt) radii [5] of the counter ions illustrates a close linear dependence of lifetimes on the Pt-Pt distance of complex neighbors. The relation does not hold for the sodium salt where another decay mechanism must be discussed.

Hexachloro complex compounds doped with Pt ions have decay constants comparable to their pure compounds (cf. Table 1 of I), indicating that energy transfer occurs between electronic levels which are predominantly located at the complex molecules. In general, somewhat longer lifetimes are expected for the doped materials compared to corresponding pure materials due to longer atomic distances between guest ions in case of statistical distribution. This is observed for the presently investigated compounds, except for $K_2SnCl_6:Pt^{4+}$, for which slightly shorter lifetimes τ_1 and τ_2 have been obtained compared to K_2PtCl_6 (see Table 1 of I). This observation is, however, not unique: also for systems such as $[Rh(en)_3](ClO_4)_3:Cr^{3+}$ and $K_3[Rh(CN)_6]:Co^{3+}$, smaller lifetimes have been reported than for the corresponding pure compounds [6, 7].

Table 2. Comparison of intrinsic lifetimes τ_0 calculated from (3), using metal spin-orbit coupling parameters as noted, with the lifetimes τ_{lim} measured at zero temperature limit from potassium salts. Reported results for some Rh(III) complexes are given as well [8].

System	ζ_μ	$\tau_0/\mu s$	$\tau_{lim}/\mu s$
PtF_6^{2-}	3550	5500	5460
$PtCl_6^{2-}$	3400	520	519
$PtBr_6^{2-}$	3100	150	86
$[RhCl_2(bpy)_2]Cl$		862	434
$[RhBr_2(bpy)_2]NO_3$		102	92.3
$[RhI_2(bpy)_2]I$		17.5	25

The main part to the decay from the first excited level at low temperature therefore can be attributed to radiative transition. Although quantum yields are not known, the very intensive red to orange red luminescence of all hexahalogeno platinates is also indicative for this.

The importance of radiative contribution to these rates can be confirmed as well by the Crosby formula relating the radiative part to the spin-orbit coupling constants ζ_i of the central ion and the ligating atoms [8]. For octahedral coordination, the rate is

$$k_{rad} = \frac{1}{\tau_0} = \frac{K}{7} \sum_{i=1}^{7} \zeta_i^2, \tag{3}$$

where K is a constant for a complex series of identical geometry. Table 2 shows the intrinsic lifetimes τ_0 calculated from (3) when using Pt(IV) spin-orbit coupling constants as indicated [9 - 11], and for the halogens F ($250\,cm^{-1}$), Cl ($600\,cm^{-1}$) and Br ($2500\,cm^{-1}$) [8-9]. The constant $K = 9.8 \cdot 10^{-4}\,sec^{-1}cm^{-1}$ is determined by an iterative procedure. The calculated numbers agree quite well with the $\tau_{l\,lim}$ from the emission experiments, confirming the preponderant radiative nature of lifetimes at measured temperatures close to zero. The disagreement obtained for the more covalent bromo complex may result from the Br coupling constant because parameters of the free ions have been used for ligands. The error allowance when calculating radiative lifetimes from (3) demonstrates corresponding results for some Rh(III) complexes in Table 2 as they were reported by Demas and Crosby [8].

Intrinsic lifetimes calculated from also oscillator strengths [12] suffer from errors resulting from the intensity integration of the absorption band which must correspond entirely to the transition in emission. In our case, the agreement with the experimental $\tau_{1\,\mathrm{lim}}$ values is not much satisfying; the trend in the halogeno series, extending over two orders of magnitude is, however, well reproduced.

2. *High Temperature Region*

The longer living terms with τ_1 and τ_2 in the lifetime curves, (13) of I, show large decreases towards higher temperature, cf. Figs. 1 to 4. This can have various reasons. Photochemical processes due to decomposition can be excluded since repeated measurements on the same sample supply equal lifetime behavior. Spontaneous emission due to vibronically induced transitions is also very improbable because in this case the temperature dependence of the radiative rate k_{rad} would follow a $\coth(\hbar\omega/2kT)$ function with ω representing a mean fundamental frequency of vibration inducing the electronic transition [13, 14]. A fitting of experimental data to this function turns out to be highly unsuccessful except for K_2PtF_6, where moderate agreement can be obtained in the low temperature region between 15 and 50 K with a parameter adjustment of $\hbar\omega = 110 \pm 5\,\mathrm{cm}^{-1}$, which is at variance with any of the fundamental metal-ligand frequencies reported for this compound [15]. Therefore, vibronical induction can also be excluded from participating in the transition mechanism.

We therefore attribute the cause of the temperature dependence to thermally activated processes due to Boltzmann population of higher excited levels. In fact, all lifetime curves of the Pt(IV) complexes in Figs. 1 to 4 can be fitted very well (by iterative least squares method) to decay functions as

$$\frac{1}{\tau_i(T)} = k_{i\,\mathrm{lim}} + \sum_l s_l^i \exp(-\Delta E_l(i)/kT) \quad (4)$$

where $k_{i\,\mathrm{lim}}$ is the temperature independent rate in the limit of $T \to 0$, i. e. $k_{i\,\mathrm{lim}} = (\tau_{i\,\mathrm{lim}})^{-1}$ as discussed before, and the $\Delta E_l(i)$ are activation energies obtained from the fitting procedure. All experimental curves can be well reproduced by (4) when for the long-living components τ_1 two or three (in case of the bromo-complex) energy depending terms are taken in the sum, and for the short-living components τ_2 only one. The result of the parameter adaptation obtained is compiled in Table 1. We conclude that activation processes extend over maximally three excited states. Since the emission intensity towards higher temperature is lower, the errors of the activation energies are relatively large. The reliability of the energy values can be checked, e. g., by comparing the results of the long- and short-living components $\Delta E(\mathrm{L})$ and $\Delta E(\mathrm{S})$, which are related to the term energies E_l (l=1, 2, ... with increasing energy), by

$$\begin{aligned} \Delta E_l(\mathrm{L}) &= E_{l+1} - E_1 \quad \text{for} \quad l = 1, 2, \\ \Delta E_1(\mathrm{S}) &= E_3 - E_2. \end{aligned} \quad (5)$$

From these equations we expect the identity

$$\Delta E_2(\mathrm{L}) - \Delta E_1(\mathrm{L}) = \Delta E_1(\mathrm{S}). \quad (6)$$

We see that this relation holds very well for K_2PtF_6 (the ΔE difference of the L component $498\,\mathrm{cm}^{-1}$ agrees with $495\,\mathrm{cm}^{-1}$ from the S component) and K_2PtCl_6 ($328\,\mathrm{cm}^{-1}$ and $320\,\mathrm{cm}^{-1}$). For the other systems, the differences are larger and their agreements are less satisfactory, which could be explained for instance by additional activation barriers arising from potential curve crossings of energy levels involved that must be surmounted when transferring energy from one level to another. The simulation of the long time component τ_1 by two exponentials in (4) and the short time component by one exponential in connection with the above energy relations strongly supports the assignment of the long-living level to the lower and the short-living level to the higher excited state.

These states are certainly not vibrational levels belonging to excited electronic states. Comparison of the activation energies from Table 1 obtained by the fitting procedure with the vibrational fundamentals reported for the Raman and IR spectra of hexahalogeno complexes [15 - 17] shows no agreements, neither qualitatively (six vibrational modes could be active) nor quantitatively (most of the ΔE_l are much larger than vibrational quanta). Moreover, deactivation from vibrational levels in general is so fast that emission from vibronically excited states to the ground state cannot be observed by the experimental equipment available to us.

The excited levels involved, therefore, must be electronic states. From the close conformity of decay constants (Table 1 of I) as well as similar activation

Table 3. Available parameter values fitted from experiments for other compounds than that in Figure 7 (identical parameter indices). Energies in cm^{-1}, rates in s^{-1}.

	ΔE_{l-1}			g_l		k_{l0}		k_{l1}			k_{l2}	
l =	2	3	4	1	2	1	2	2	3	4	3	4
K_2PtCl_6	97	425		2	3	$1.9 \cdot 10^3$	$2 \cdot 10^3$	$5 \cdot 10^3$	$1 \cdot 10^5$	·	$\sim 10^5$	·
K_2PtBr_6 (site A)	162	853	1535	2	3	$5.8 \cdot 10^2$	·	$3 \cdot 10^4$	$\sim 10^8$	$\sim 10^{11}$	·	·
K_2PtBr_6 (site B)	146	816	>1500	2	3	$1.4 \cdot 10^3$	·	$\sim 10^4$	$\sim 10^8$	$> 10^{11}$	·	·

energies ΔE_i (Table 1 of this work) for pure and corresponding doped complexes we conclude, as mentioned, that these levels are molecular states predominantly localized at individual Pt(IV) complex units. The activation energies then correspond in fair approximation to energy differences between electronic levels in the term scheme of molecular complexes (see Fig. 7 and listings in Table 3). Since the τ_3 component of K_2PtF_6 is temperature independent over the whole range investigated (cf. Fig. 1), the next higher energy level $i = 4$ over those plotted in Fig. 7 must lie more than $800\,cm^{-1}$ above $\Gamma_3(^3T_{1g})$, which cannot be thermally occupied.

The $\Delta E_l(i)$ parameters obtained from the fit to (4) are, however, generally smaller than the energy differences derived from absorption spectra, because the latter refer to Franck-Condon transitions starting from nuclear configurations of the ground state, while energies obtained from emission spectra are those resulting from the equilibrium geometry of the excited states. Since corresponding potential curves are expected to be shifted due to the change of orbital occupation from t_{2g}^6 to $t_{2g}^5 e_g$, the excited and the ground state have different geometry. Also, activation energy to higher level occupation may contribute to varying ΔE_l parameters. The energies derived from absorption spectra of Pt^{4+} doped in Cs_2GeF_2 are $\Delta E_1 = 839\,cm^{-1}$ and $\Delta E_2 = 2539\,cm^{-1}$ [15], for K_2PtCl_6 $\Delta E_1 = 900\,cm^{-1}$ and $\Delta E_2 = 1000\,cm^{-1}$ [10]. Although they differ considerably from the present life time measurements, the level sequence $\Gamma_3 < \Gamma_5 < \Gamma_4$ in both cases is identical. We also carried out temperature dependent luminescence spectra [18]. From 20 to 200 K the emission band of all halogeno complexes loses the vibrational fine structure and assumes a broad band with a maximum shifting in case of K_2PtCl_6 from 15035 to $15450\,cm^{-1}$. Since the emission intensity decreases drastically with temperature, band analyses for determining energies of more than one emitting state cannot be carried out. Also quantum chemistry calculations of excited states for different metal-ligand atomic distances supporting the present views are not possible with sufficient accuracy.

The rates k_{lm} between levels l and m are defined, from the rate equations of an N-level system which describe the relaxation of the excited level l with occupation number n_l, by [19]

$$\frac{dn_l}{dt} = \sum_{m \neq l}^{N-1} (-k_{lm} n_l + k_{ml} n_m), \quad l = 0, \ldots, N-1. \tag{7}$$

The number of parameters can be reduced when assuming detailed balance relations between transition rates k_{lm} and k_{ml}, yielding [20, 21]

$$k_{lm} = k_{ml} \frac{g_l}{g_m} \exp(-\Delta E_{lm}/kT), \tag{8}$$

where ΔE_{lm} is the energy gap between levels l and m, and g_l, g_m are their degrees of degeneracy. Moreover, the k_{l0} parameters are known from limits $\tau_{i\,\mathrm{lim}}$ for $T \to 0$ which are different for long ($i = 1$) and short ($i = 2$) components (see above). The other k_{lm} and the degeneracies are calculated by fitting the roots $1/\tau_i$ of the characteristic equation belonging to (7) to the experiment. This procedure is quite common in the case of a 3-level system, for which the solutions are given in analytical form [20 - 22]. For a higher level system the evaluation uses iterative procedures leading to approximate solutions. Orders of magnitude are obtained from the s_l coefficients of (4), which become respective rate constants for $T \to \infty$ and $k_{lm} \geq k_{l0}, k_{m0}$. For determining degeneracies, several trial calculations with different g_l parameter sets have been carried out to obtain maximal agreement with the experimental data from the Arrhenius curves. In all cases, the degeneracy numbers agree with the level degeneracies derived from absorption spectra and from energy level calculations which include spin-orbit coupling [10, 15]. Results, as far as

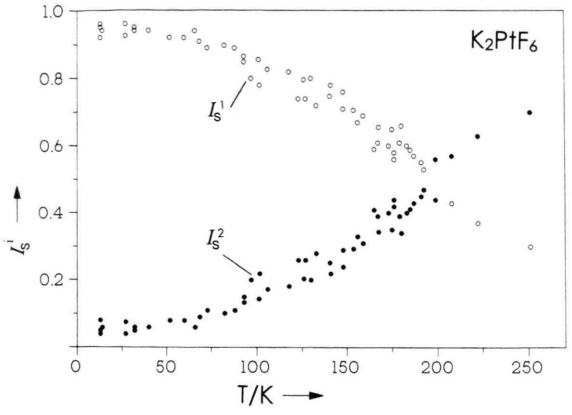

Fig. 9. Temperature dependence of saturation limits I_S^1 of the long time decay component and I_S^2 of the short time component measured from K_2PtF_6.

they could be calculated with some reliability, are compiled in Table 3.

A further indication for thermal population of higher excited levels is the above mentioned blue shift of luminescence bands with increasing temperature which is observed in the region higher than 100 K [18]. Parallel to this, the saturation limit of intensity I_S^1 for the long time component is decreased at higher temperature in favor of I_S^2 for the short time component (for definition see part I). Figure 9 illustrates these changes very well in the case of K_2PtF_6.

3. *Phase Transitions and Multiple Sites*

The Arrhenius diagram of K_2PtBr_6 (Fig. 4) shows a discontinuity for both lifetimes τ_1 and τ_2 occurring within a small range of temperature. The long time component τ_1, for instance, increases between 32 and 37 K from 86 to 1 860 µs. Below 30 K, a bi-exponential decay, above 37 K a tri-exponential decay curve is obtained from the fitting procedure. The temperature dependence is non-chaotic in the temperature regions below and above, supplying reasonable parameter values for lifetimes and activation energies. This indicates a phase transition of the crystal at a temperature between 32 and 37 K, changing the environment of Pt(IV) chromophores in such a way that the radiative decay kinetics is different. Several other phase transitions have been reported from thermal analysis of K_2PtBr_6 (space group at normal conditions is Fm 3m) at temperatures between 78 and 169 K [23, 24]. A further phase change may occur at lower temperature which, to our knowledge, has not been observed so far. Far infrared spectra recorded at 10 K and 40 K on a Bruker Fourier transform instrument IFS 113 ν show absorption band changes below 50 cm^{-1} energy, i. e.only in the region of lattice vibrations that is indicative for a phase transition [18].

The results obtained from K_2PtBr_6 are different from the other Pt compounds investigated in another respect: the tri-exponential decay yields three different lifetime parameters τ_1 to τ_3, and the Arrhenius fit carried out for two of the diagrams above the phase transition temperature (the third cannot be evaluated because of large uncertainties due to low intensity, cf. Figure 4) supplies very similar activation energies ΔE_1 and ΔE_2 for the lifetimes τ_1 and τ_2 (cf. Table 1). These data can be explained by the presence of at least three inequivalent sites A, B, and C in the crystal lattice (indications for similar ΔE_3 values are also obtained from the τ_3 decay component). The chromophores on these sites, therefore, have comparable energy level schemes, but due to the large sensitivity of lifetimes caused by the environment they decay differently.

The time resolved spectrum at 12 K of Fig. 5 shows emission from two levels of different lifetimes, which according to the peak shift differ in energy by 146 cm^{-1}. This number agrees well with the ΔE_1 values of Table 3 obtained for sites A and B valid for temperatures higher than 35 K. While the level energies of the complex molecules are not changed very much by the phase transition, it is the environment which is responsible for the differences in lifetime.

A further increase of temperature does not show any other unsteady changes of lifetimes although some more phase transitions have been reported for K_2PtBr_6 at higher temperature [23, 24]. The absence may be explained by increased non-radiative transitions, also through other channels playing a role at higher temperature, which are known to be less sensitive with respect to environmental changes [25].

In a real crystal, the complexes occupy in general sites which are, although being crystallographically equivalent, only approximately equal, which for instance gives rise to inhomogeneous line broadening. Since varying environments lead to different time dependences of luminescence, we expect for an arbitrary distribution of sites with more or less distorted neighborhoods a large number of different lifetimes of similar size which are Gaussian distributed around a maximum that represents the mean value. James and Ware [26] pointed out that multiexponential decay with normal distributed lifetime parameters can be

falsely interpreted as bi-exponential decay from evaluating experimental lifetime curves. We have checked this by calculation and found that a decay function of only seven exponentials with normal distributed lifetimes τ_i and intensity limits I_S^i (see I) yielding a gaussian distribution indeed can be fitted very well to a bi-exponential decay function supplying a test statistics which is within the limits for non-rejection of the model function (cf. I). Therefore a distinction between multi- and bi-exponential decay in principle could not be possible. Further evaluations should be carried out. In our case we have looked into the τ-distributions measured for K_2PtCl_6, considering a larger series of exponentials in the decay curve, registering the lifetimes τ_i ($i = 1, 2, \ldots$) at varying temperatures. We could show that most of these lifetimes lead to chaotic temperature dependences in the Arrhenius plot which, as we mentioned in I, is a matter of rejection of multi-exponential functions for this compound.

Conclusions

The relative size of decay parameters obtained for the present Pt(IV) complexes is somewhat different to most of other transition metal compounds, which has its origin in the emissions of several excited states with relatively close lying energies. The rate parameters k_{lm} between the excited levels l and m are in some cases only slightly larger than the rates k_{l0} to the ground state, and the neighboring energy level differences ΔE_{lm} are found between 70 to 800 cm^{-1} for the first three excited states. Even at 2 K the decay is poly-exponential for all compounds investigated.

Emission of $K_3Co(CN)_3$, for comparison, also occurs from several excited states (spin-orbit levels of $^3T_{1g}$). The decay curve is, however, mono-exponential (see I) also at higher temperature because the kinetics between the excited levels is much faster than the deactivation to the electronic ground state. Rates between excited states of Co(III) and Rh(III) complexes are reported being of the order of $10^{10}s^{-1}$ [27, 28].

On the other hand, if emission from higher excited states is apparent from the lifetime curves, the energy difference between the excited states should be larger than a certain number of vibrational quanta bridging the energy gap [2 - 4]. In this case the transition probability for radiationless transitions is only a minor part of the measured k_{l0} rates, and the k_{lm} between the emitting levels can be neglected. Emission resulting from different excited states violating Kasha's rule is eventually observed in different energy regions. Well known examples for complex compounds of this kind are Re(IV)d^3, Os(IV)d^4 and Ni(II)d^8 complexes [29 - 31].

The situation for Pt(IV) compounds, as we see, seems to be in part different. It fits neither completely into the picture for fast interexcited state kinetics nor into that for large energy differences. The reason for the slow kinetics between close lying excited states probably results from more strictly obeyed selection rules between excited states inferred from different spin-orbit coupling and crystal symmetry effects, such that the transition probability regime proves to be superior to the thermal equilibrium regime [32].

Acknowledgement

Financial support of the Fonds der Chemischen Industrie, Frankfurt/Main, is acknowledged.

[1] I. Biertümpel und H.-H. Schmidtke, Chem. Phys. **215**, 271 (1997).
[2] B. Henderson and G. F. Imbusch, Optical Spectroscopy of Inorganic Solids, Clarendon Press, Oxford 1989.
[3] K. Kühn, F. Wasgestian, and H. Kupka, J. Phys. Chem. **85**, 665 (1981).
[4] A. Ditze and F. Wasgestian, Ber. Bunsenges. Phys. Chem. **90**, 111 (1986).
[5] Handbook of Chemistry and Physics, 66 ed., F 164, CRC Press Inc., Boca Raton 1985/6.
[6] A. Wölpl and D. Oelkrug, Ber. Bunsenges. Phys. Chem. **79**, 394 (1975).
[7] H.-H. Schmidtke, I. Biertümpel, and J. Degen, Ber. Bunsenges. Phys. Chem. **93,** 1485 (1989).
[8] J. N. Demas and G. A. Crosby, J. Amer. Chem. Soc. **92**, 7262(1970) and **93**, 2841 (1970).
[9] T. R. Thomas, R. J. Watts, and G. A. Crosby, J. Chem. Phys. **59**, 2123 (1973).
[10] G. Eyring, T. Schönherr, and H.-H. Schmidtke, Theoret. Chim. Acta **64**, 83 (1983).
[11] M. P. Laurent, H. H. Patterson, W. Pike, and H. Engstrom, Inorg. Chem. **20**, 372 (1981).
[12] V. Balzani and V. Carassiti, Photochemistry of Coordination Compounds, Academic Press, London 1970.

[13] S. M. Healy, C. J. Donnely, T. J. Gynn, G. F. Imbush, and G. P. Morgan, J. Lumin. **46**, 1 (1990).
[14] C. Reber and H. U. Güdel, J. Lumin. **47**, 7 (1990).
[15] H. H. Patterson, W. J. De Berry, J. E. Byrne, and M. T. Hsu, Inorg. Chem. **16**, 1698 (1977).
[16] K. P. Balashev, Sov. J. Coord. Chem. (Engl. Transl.) **15**, 73 (1989).
[17] G. Eyring and H.-H. Schmidtke, Ber. Bunsenges. Phys. Chem. **85**, 597 (1981).
[18] I. Biertümpel, Thesis, Heinrich-Heine-Universität, Düsseldorf 1993.
[19] B. DiBartolo, Optical Interactions in Solids, John Wiley, New York 1968.
[20] H.-H. Schmidtke, M. Bosenbeck, and J. Degen, J. Lumin. **44**, 177 (1989).
[21] J. Degen and H.-H. Schmidtke, Chem. Phys. **129**, 483 (1989).
[22] T. J. Kemp, Progr. Reaction Kinetics **10**, 301 (1980).
[23] K. Rössler and J. Winter, Chem. Phys. Lett. **46**, 566 (1977).
[24] R. W. Berg, J. Chem. Phys. **71**, 2531 (1979).
[25] L. S. Forster, Chem. Rev. **90**, 331 (1990).
[26] D. R. James and W. R. Ware, Chem. Phys. **120**, 455 (1985).
[27] J. N. Demas, J. Chem. Educ. **60**, 803 (1983).
[28] D. Magde, G. E. Rojas, and L. H. Skibsted, Inorg. Chem. **27**, 2900 (1988).
[29] H.-H. Schmidtke and R. Wernicke, Chem. Phys. Lett. **40**, 339 (1976).
[30] C. D. Flint and A. G. Paulusz, Mol. Phys. **41**, 907 (1980).
[31] P. S. May and H. U. Güdel, J. Lumin. **46**, 277 (1990).
[32] H.-H. Schmidtke, M. Diehl, and J. Degen, J. Phys. Chem. **96**, 3605 (1992).